Circuits & Power Grids

Advanced Topics in Control 2017: Distributed Systems & Control

Florian Dörfler

In this lecture we demonstrate how various tools acquired in the previous sections can be used to analyze circuits. Conversely, we will also show how concepts from circuit theory such as effective resistance again inform network and graph theory. In fact, history took the reverse path, that is, a lot of modern algebraic graph theory as well as network dynamics grew out of circuit analysis. In fact, Kirchhoff is by many regarded as one of the first graph theoreticians.

We will show how the insights from circuit theory can be constructively used to design controllers for stand-alone DC power grids. These control strategies are prototypical for distributed control over undirected graphs and can be used analogously in robotic coordination and other applications.

1 Circuit modeling

Consider a circuit composed of $n+1$ nodes $\mathcal{V} \in \{1, \dots, n\} \cup \{0\}$ and m undirected edges $\mathcal{E} \subset \mathcal{V} \times \mathcal{V}$, which are often referred to as buses and branches in circuit theory and the power systems/electronics literature. The 0-node is the common electrical ground, which is typically treated as a separate node. We associate with each node $i \in \{1, \dots, n\} \cup \{0\}$

- a nodal current injection $I_i \in \mathbb{R}$, and
- a potential (sometimes also referred to as a nodal voltage) $V_i \in \mathbb{R}$.

Let us choose an arbitrary orientation for each undirected edge $\{i, j\} \in \mathcal{E}$, and define for each associated directed edge (i, j)

- a directed current flow $f_{ij} \in \mathbb{R}$, and
- a directed voltage $u_{ij} \in \mathbb{R}$.

Our notation in this section follows the convention that nodal variables are denoted by capital letters whereas edge variables are denoted by lower case letters.

Fundamental laws: The topology of the circuit is encoded by the associated (oriented) incidence matrix $B \in \mathbb{R}^{n \times m}$ which relates the nodal variables and the edge variables by Kirchhoff's laws:

(i) Kirchhoff's current law (KCL): $I_i = \sum_{j \in \mathcal{N}(i)} f_{ij}$ for all $i \in \{1, \dots, n\} \cup \{0\}$. Equivalently, in vector form we have $I = Bf$.

(ii) Kirchhoff's voltage law (KVL): $0 = \sum_{\{i,j\} \in \text{cycle } k} u_{ij}$ for all distinct cycles $k \in \{1, \dots, m - n + 1\}$. Equivalently, in vector form we have $u = B^T V$.

Kirchhoff's two laws define $n+m$ linear equations relating the $2n+2m$ variables (V, I, f, u), and they need to be complemented by further equations relating these quantities through impedance laws for any pair of connected nodes $\{i,j\} \in \mathcal{E}$. According to the least action principle (see exercise E6.13), the impedance law for a resistor is given by Ohm's law and in general case as follows:

(iii) Impedance laws:

- Resistor (Ohm's law): $u_{ij} = r_{ij} f_{ij}$, where $r_{ij} > 0$ is a resistance;
- Inductor (Faraday's law): $l_{ij} \frac{d}{dt} f_{ij} = u_{ij}$, where $l_{ij} > 0$ is an inductance; and
- Capacitor (charge balance): $c_{ij} \frac{d}{dt} u_{ij} = f_{ij}$, where $c_{ij} > 0$ is a capacitance.

The three devices are illustrated with their circuit symbols in Figure 1.

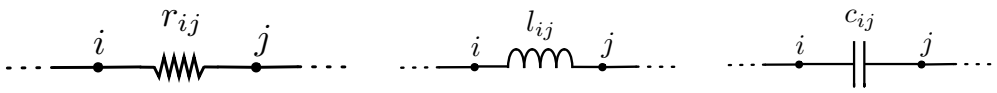

(a) resistive branch (b) inductive branch (c) capacitive branch

Figure 1: Circuit symbols for resistors, inductors, and capacitors

Ground, load, and source models: Observe that Kirchhoff's laws and the impedance laws define the potential v only up to an arbitrary reference. Often it is convenient to define the potential of the electrical ground as zero-valued: $v_0 = 0$. In this case, an resistor r_{i0} to ground draws a current $f_{i0} = V_i(s)/r_{i0}$ and we drop the index "0" henceforth.

(iv) Ground: the ground has zero potential $V_0 = 0$ and we drop the index "0" in r_{i0}, l_{i0}, c_{i0}

For example, a resistor r_i to ground is often used to model a load connected to node i. These are often termed *shunt resistors*. Whereas a resistor draws a current $i_{i0} = V_i/r_i$, another popular load or device model is a *constant current demand* $I_i^* \in \mathbb{R}_{\leq 0}$ as depicted in Figure 2(a). The overall current injection at node i is then $I_i = I_i^* - V_i/r_i$.

Ideal sources can be modeled in a similar way:

(v) Sources: a device that provides a constant current injection $I_i^* \in \mathbb{R}_{\geq 0}$ or a constant potential $V_i^* \in \mathbb{R}_{\geq 0}$ at node i is termed an *ideal current source* or an *ideal voltage source*, respectively.

An ideal current source and voltage source are depicted in Figure 2(b). We show those in combination with a resistor r_i to ground and with a series resistance r_{ik}, respectively, for the following reason: By Ohm's law these two models are equivalent upon equalizing $r_i = r_{ki}$. Thus, an ideal voltage source can always be converted to an ideal current source and vice versa. In the following, we focus without loss of generality on constant current sources.

Kirchhoff's laws, the impedance laws, and the models for loads and sources provide all ingredients to model a linear circuit. Nonlinear circuits can be modeled by means of nonlinear impedance laws specifying more general relationships between the variables u_{ij}, f_{ij}, and their derivatives.

2 Different branch models

In the following, we combine Kirchhoff's laws and the models for loads and sources together with different prototypical models for the branch impedances, as depicted in Figure 3.

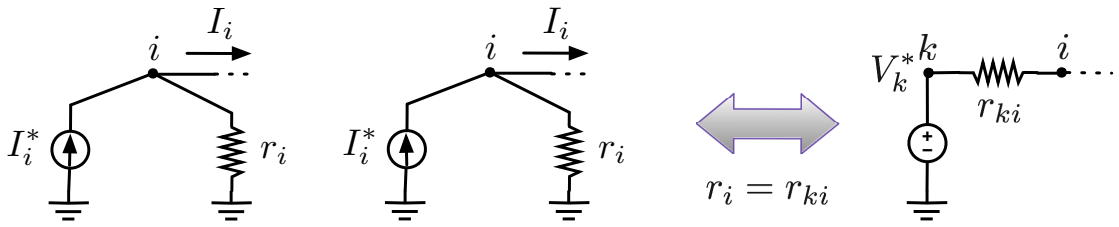

(a) Constant current load and resistive load

(b) Equivalent constant current and constant voltage sources

Figure 2: Circuit elements with connections to ground. Observe our sign convention: for a constant current load $I_i^* \leq 0$ whereas for an ideal current source $I_i^* \geq 0$.

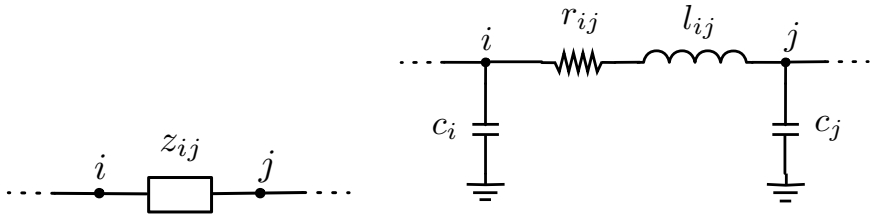

(a) complex impedance

(b) Π-model of a circuit branch

Figure 3: More complex branch models

Purely resistive circuits: If all branches are purely resistive as depicted in Figure 1(a), then Kirchhoff's and Ohm's laws lead to

$$I = Bf = B\text{diag}(1/r_{ij})u_{ij} = B\text{diag}(1/r_{ij})B^T V \tag{1}$$

or $I = LV$, where $L = B\text{diag}(1/r_{ij})B^T$ is the circuit conductance matrix, that is, a Laplacian matrix induced by the adjacency matrix with elements $1/r_{ij}$. If node i has a constant current injection I_i^* (positive for a source and negative for a load) and a shunt resistance r_i drawing a current V_i/r_i as in Figure 2(a), then $I_i = I_i^* - V_i/r_i$, and the overall circuit equations read as

$$I^* = \left(B\text{diag}(1/r_{ij})B^T + \text{diag}(1/r_i)\right) V\,. \tag{2}$$

It can be verified that the matrix $B\text{diag}(1/r_{ij})B^T + \text{diag}(1/r_i)$ in (2) is positive definite provided that at least one shunt resistor is present; see Exercise 10. In Chapter 9, we will identify the matrix $B\text{diag}(1/r_{ij})B^T + \text{diag}(1/r_i)$ as a Hurwitz Metzler matrix and show various proporties; for example its inverse is positive; see Theorem 9.5

Complex-valued impedances: Often linear circuits are modeled in the Laplace s-domain by taking Laplace transforms of the impedance laws. In this case the linear impedance laws reads as

$$u_{ij}(s) = z_{ij}(s) f_{ij}(s),$$

where $z_{ij}(s)$ is the line impedance, as depicted in Figure 3(a). For example, for an inductive branch Faraday's law reads as $u_{ij}(s) = s \cdot l_{ij} f_{ij}(s)$. More general line impedances, for example, the Π-model in Figure 3(b) can be aggregated in an impedance transfer function $z_{ij}(s)$.

By analogous calculations as in the resistive case, we arrive at $I(s) = Y(s)V(s)$, where $Y(s) = B\mathrm{diag}(1/z_{ij}(s))B^T$ is the circuit admittance matrix, and its pseudo inverse (as calculated in exercise E6.8) $Z(s) = Y(s)^\dagger$ is the so-called *impedance matrix*. With general complex-valued load and source models and complex-valued shunt impedances $z_i(s)$ to ground, we arrive (analogous to (1)) at

$$I^*(s) = \left(B\mathrm{diag}(1/z_{ij}(s))B^T + \mathrm{diag}(1/z_i(s))\right) V(s)\,.$$

Π-model: The popular Π-model [9] of a branch is depicted in Figure 3(b). The Π-model can be used to model various line characteristics from high-voltage transmission lines to low-voltage underground cables. It consists of a series resistive-inductive impedance modeling the line inductance and losses as well as a shunt capacitor to ground at each end of the line modeling the line charging. Typically, the two shunt capacitors take identical values. Note that if there are multiple branches connected to a node, each modeled by the Π-model, there will be multiple parallel shunt capacitors which we can combine into a single one.

3 A prototypical circuit

In the following, we consider a prototypical circuit model as it is encountered in many power distribution and transmission grids. We model each line by the Π-model as in Figure 3(b). At each node we consider a load/source model in terms of a constant current injection I_i^* and a shunt resistance constant resistance r_i at each node $i \in \{1, \dots, n\}$. In this case, the circuit equations are

$$\begin{aligned}
&\text{KCL:} && I = Bf\,, && \text{(3a)}\\
&\text{KVL:} && u = B^T V\,, && \text{(3b)}\\
&\text{Ground model:} && I = I^* - C\dot{V} - GV\,, && \text{(3c)}\\
&\text{Branch model:} && L\dot{f} = u - Rf\,, && \text{(3d)}
\end{aligned}$$

where R, L, C, G are diagonal matrices of c_i, r_{ij}, l_{ij}, and $g_i = 1/r_i$, and $I^* = (I_1^*, \dots, I_n^*)$ is a constant external current injections modeling, e.g., an ideal current source or or a constant current load.

It is convenient to reduce the circuit equations (3) to a state space model that is defined only in terms of the variables v and f associated to capacitive and inductive storage elements. By inserting (3a) and (3b) in (3c) and (3d), respectively, we obtain

$$\begin{bmatrix} C & \\ & L \end{bmatrix} \begin{bmatrix} \dot{V} \\ \dot{f} \end{bmatrix} = \underbrace{\left(\begin{bmatrix} & -B \\ B^T & \end{bmatrix} - \begin{bmatrix} G & \\ & R \end{bmatrix} \right)}_{=Q} \begin{bmatrix} V \\ f \end{bmatrix} + \begin{bmatrix} I^* \\ \mathbb{O}_m \end{bmatrix}. \tag{4}$$

A block-diagram of the circuit model (3), respectively, (4), is shown in Figure 4. Notice the separation of the node and edge dynamics as well as the similarity to the block-diagrams in Figure 8.1 (consensus), Figure E8.1 (relative sensing networks), and Figure 13.2 (potential-based relative motion control) arising in other applications.

Noteworthy special cases: The purely resistive circuit equations (2) can be recovered from the model (4) in the limit $L \to 0$ and $C \to 0$ so that $I^* = Bf + GV$ and $Rf = B^T V$ which can be combined to $I^* = BR^{-1}B^T V + GV$. The latter again equals equation (2).

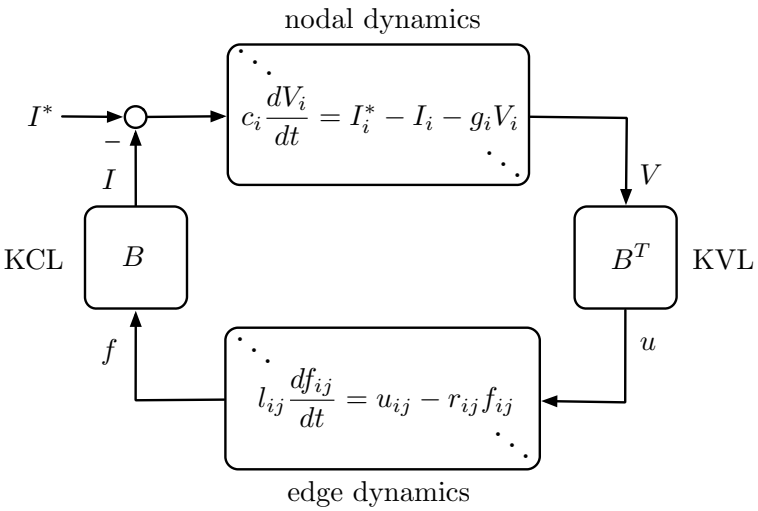

Figure 4: Block-diagram of the circuit model (3)

In absence of constant current injections and dissipative elements, that is, for $I^* = \mathbb{0}_n$, $G = \mathbb{0}$ and $R = \mathbb{0}$, and for $C = I_n$, the Π-model reduces to the Laplacian oscillator (see Exercise 1)

$$\ddot{V} = -\mathcal{L}_L V\,, \tag{5}$$

where $\mathcal{L}_L = BL^{-1}B^T$ is the inverse-inductance-weighted Laplacian of the underlying circuit.

In case that the circuit branches are made of the same material and thus the ratio of $l_{ij}/r_{ij} = \tau$ is constant for all edges $\{i,j\} \in \mathcal{E}$, then it can be shown (see Exercise 1) the circuit model (3) reduces to a second-order consensus-type model:

$$\tau C\ddot{V} + (\tau G + C)\dot{V} + (\mathcal{L}_R + G)V = I^*\,, \tag{6}$$

where $\mathcal{L}_R = BR^{-1}B^T$ is the conductance matrix. Indeed, for $\tau = 1$, $C = I_n$, $G = \mathbb{0}$, and $I^* = \mathbb{0}_n$ we recover the standard second-order Laplacian flow from (6):

$$\ddot{V} + \dot{V} + \mathcal{L}_R V = \mathbb{0}_n\,.$$

On the other hand, for $\tau = 0$ and $C = I_n$, $G = \mathbb{0}$, $I^* = \mathbb{0}_n$ as before, we recover the standard Laplacian flow

$$\dot{V} = -\mathcal{L}_R V\,.$$

4 Circuit analysis based on energy methods

The matrix Q in the circuit equations (4) contains many structural features that are unveiled when considering the electric as well as the magnetic energy associated to the storage elements:

$$\mathcal{H}(V,f) = \frac{1}{2}V^T C V + \frac{1}{2}f^T L f\,. \tag{7}$$

The derivative of the energy function (7) along trajectories of (9) is given by the *power balance*

$$\dot{\mathcal{H}}(V,f) = \underbrace{\begin{bmatrix} V \\ f \end{bmatrix}^T \begin{bmatrix} & -B \\ B^T & \end{bmatrix} \begin{bmatrix} V \\ f \end{bmatrix}}_{=0 \text{ (lossless power circulations)}} \underbrace{- \begin{bmatrix} V \\ f \end{bmatrix}^T \begin{bmatrix} G & \\ & R \end{bmatrix} \begin{bmatrix} V \\ f \end{bmatrix}}_{\leq 0 \text{ (power losses)}} \underbrace{+V^T I^*}_{\text{(power supplied)}}\,.$$

The last term in the above power balance equation corresponds to the external power supplied to the circuit through the current injections, the central term corresponds to dissipation induced by shunt and branch resistances, and the first term evaluating to zero due to skew-symmetry of matrix in the quadratic form. To unveil the role of the first term, we consider a circuit without dissipation or exogenous current injections. The following lemma shows that the dynamic behavior is governed by lossless energy exchange between the inductive and capacitive storage elements. Thus, the first term corresponds to lossless power circulations between the storage elements.

Lemma 4.1 (Circulations in non-dissipative circuit). *Consider system (4) with $I^* = \mathbb{0}_n$, $G = \mathbb{0}$, $R = \mathbb{0}$. The solution is a superposition of n undamped harmonic signals. Moreover, if $C = I_n$, then the frequencies of these harmonics are $\sqrt{\lambda_i}$, $i \in \{1, \dots, n\}$, where λ_i are the eigenvalues of the inverse-inductance-weighted network Laplacian matrix $\mathcal{L}_L = BL^{-1}B^T$.*

Proof. In case that $I^* = \mathbb{0}_n$, $G = \mathbb{0}$, and $R = \mathbb{0}$ the circuit model (4) reduces to

$$\begin{bmatrix} C & \\ & L \end{bmatrix} \begin{bmatrix} \dot{V} \\ \dot{f} \end{bmatrix} = \begin{bmatrix} & -B \\ B^T & \end{bmatrix} \begin{bmatrix} V \\ f \end{bmatrix} . \tag{8}$$

The system (8) defines an oscillator in (V, f)-space since the level sets (ellipsoids) of the energy function (7) are invariant: $\dot{\mathcal{H}}(V, f) = 0$. Thus, the level sets of $\mathcal{H}(V, f)$ are the images of oscillating trajectories $(V(t), f(t))$ satisfying $\mathcal{H}(V(t), f(t)) = \mathcal{H}(V_0, f_0)$ for all $t \geq 0$.

For $C = I_n$, the system (8) may be equivalently be written as the *Laplacian oscillator* in (5):

$$\ddot{V} = -B\dot{f} = -BL^{-1}B^T V = -\mathcal{L}_L V \,,$$

Let (λ_i, w_i) be an eigenvalue and eigenvector pair of the Laplacian $\mathcal{L}_L$, then for each mode $i \in \{1, \dots, n\}$, we can insert $V = w_i$ in the Laplacian oscillator equation (5) and obtain

$$\ddot{w}_i = -\lambda_i w_i \,, \qquad i \in \{1, \dots, n\} \,,$$

that is, $w_i(t)$ is a harmonic signal of the form $w_i(t) = A_i \cos(\sqrt{\lambda_i} t + \varphi_i)$ of frequency $\sqrt{\lambda_i}$, where the amplitude A_i and a phase shift φ_i are determined from the initial conditions $(w_i(0), \dot{w}_i(0))$. Hence, $V(t) = \sum_{i=1}^n w_i(t)$ is a superposition of n harmonic signals with frequencies $\sqrt{\lambda_i}$, $i \in \{1, \dots, n\}$. □

In the following, we study the fully dissipative case, where all branch and shunt elements have resistive contributions.

Lemma 4.2 (Convergence in fully dissipative circuit). *Consider system (4) with $I^* \in \mathbb{R}^n$ and positive definite matrices of shunt and branch resistances G and R. The system admits a globally exponentially stable equilibrium point whose location depends on the constant current injections I^*.*

Proof. We begin by studying the equilibria of (4). Observe that the Q-matrix is composed of a skew-symmetric minus a positive definite matrix. Thus $Q + Q^T$ is negative definite, Q is Hurwitz and thus invertible. Hence, there exists a unique equilibrium $[V^* \; f^*]^T = -Q^{-1} [I^* \; \mathbb{0}_m]^T$ that depends on the external current injections I^*. The fact that Q is Hurwitz implies that (V^*, f^*) is globally exponentially stable; see Exercise E7.2.

This fact can also be proved with a Lyapunov argument that extends to nonlinear circuit models. Consider the incremental error coordinates $(\tilde{V}, \tilde{f}) = (V - V^*, f - f^*)$ and rewrite the model (4) as

$$\begin{bmatrix} C & \\ & L \end{bmatrix} \begin{bmatrix} \dot{\tilde{V}} \\ \dot{\tilde{f}} \end{bmatrix} = \underbrace{\left(\begin{bmatrix} & -B \\ B^T & \end{bmatrix} - \begin{bmatrix} G & \\ & R \end{bmatrix} \right)}_{=Q} \begin{bmatrix} \tilde{V} \\ \tilde{f} \end{bmatrix} \tag{9}$$

Akin to the energy function (7), consider the incremental electric as well the incremental magnetic energy as a Lyapunov function candidate

$$\mathcal{H}(\tilde{V},\tilde{f}) = \frac{1}{2}\tilde{V}^T C\tilde{V} + \frac{1}{2}\tilde{f}^T L\tilde{f} \tag{10}$$

whose derivative along trajectories of (9) is given by

$$\dot{\mathcal{H}}(\tilde{V},\tilde{f}) = \begin{bmatrix}\tilde{V}\\ \tilde{f}\end{bmatrix}^T Q \begin{bmatrix}\tilde{V}\\ \tilde{f}\end{bmatrix} = -\begin{bmatrix}\tilde{V}\\ \tilde{f}\end{bmatrix}^T \begin{bmatrix}G & \\ & R\end{bmatrix} \begin{bmatrix}\tilde{V}\\ \tilde{f}\end{bmatrix} = \begin{cases} = 0 & \text{if } (\tilde{V},\tilde{f}) = \mathbb{0}_{n+m} \\ < 0 & \text{else}\end{cases},$$

where we made use of the skew-symmetry of Q. By Lyapunov's theorem (Theorem 13.4), the equilibrium (V^*, f^*) is asymptotically stable (globally exponentially stable to be precise). □

Notice that the stability conclusion in Lemma 4.2 is oblivious of the actual underlying network topology as encoded in the B matrix. The network affects only the location of the equilibria. Of course, this somewhat surprising result is a consequence of the fact that the network is considered to be fully dissipative in Lemma 4.2. Consider now the cases that either $G = \mathbb{0}$ or $R = \mathbb{0}$. In these cases the equilibria of (4) satisfy either $B^T V = \mathbb{0}_m$ or $Bf = \mathbb{0}_n$, respectively. In words, nodal voltages reach consensus $B^T V = \mathbb{0}_m$ and are defined up to a translation, or the currents converge to the cycle space $Bf = \mathbb{0}_n$ and are defined up to a circulating current; see Section 8.4.

Lemma 4.3 (Convergence in partially dissipative circuit). *Consider system (4) with $I^* = \mathbb{0}_n$ and matrices of shunt and branch resistances $G \in \mathbb{R}^{n\times n}$ and $R \in \mathbb{R}^{m\times m}$.*

1. *If $R = \mathbb{0}$ and G is positive definite, then all trajectories converge asymptotically to stationary solutions in the equilibrium subspace $(V^*, f^*) \in (\mathbb{0}_n, \text{kernel}(B))$, that is, the equilibria are uniquely defined up to a subspace corresponding to circulating currents $f^* \in \text{kernel}(B)$.*
2. *If $G = \mathbb{0}$ and R is positive definite, then all trajectories converge asymptotically to stationary solutions in the equilibrium subspace $(V^*, f^*) \in (\text{span}(\mathbb{1}_n), \mathbb{0}_m)$, that is, the nodal voltages V^* reach consensus and are defined up only to an arbitrary reference.*

We refer to the solution of Exercise 2 for the proof details which rely on properties of saddle matrices as discussed in Lemma 7.5.

5 Effective resistance

In the following, we are interested in analyzing properties of steady-state circuits – in particular, the notion of effective resistance has a close connection to various concepts that we studied before. Consider a static (steady-state) circuit model with resistive branch connections and a connected graph. Assume without loss of generality that the circuit has no shunt elements as these can be modeled as branch connections to the 0-node. Hence, the circuit equations are given as in (1) by

$$I = LV \tag{11}$$

where $I \in \mathbb{R}^n$ and $V \in \mathbb{R}^n$ are the vectors of current injections and potentials, and $L = \mathcal{L}_R \in \mathbb{R}^{n\times n}$ is the Laplacian matrix of the graph with weights $1/R_{ij}$ between a connected pair of nodes $\{i,j\} \in \mathcal{E}$.

Definition 5.1 (Effective resistance). *Consider an undirected, connected, and weighted graph. The effective resistance r_{ij}^{eff} between any pair of (not necessarily neighboring) nodes $i, j \in \{1,\dots,n\}$ is defined as the potential difference between the nodes i and j when a unit current is injected in i and extracted in j; see Figure 5 for an illustration.*

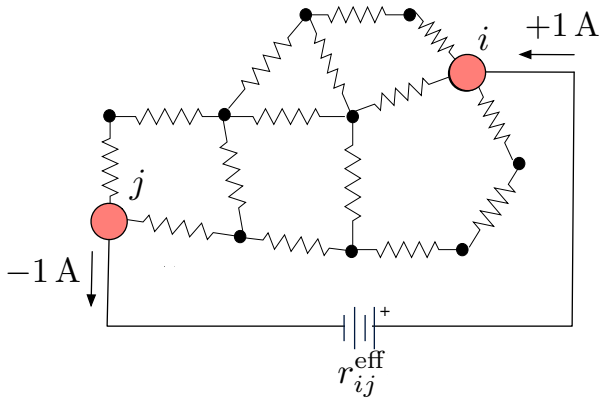

Figure 5: The effective resistance between nodes i and j is the potential difference when a unit current of 1 A is injected in i and extracted in j.

Lemma 5.2 (**Calculation of the effective resistance**). *The effective resistance r_{ij}^{eff} between two nodes $i, j \in \{1, \dots, n\}$ of an undirected, connected, and weighted graph with Laplacian matrix L can be obtained as*

$$r_{ij}^{\text{eff}} \triangleq (e_i - e_j)^T L^\dagger (e_i - e_j) = L_{ii}^\dagger + L_{jj}^\dagger - 2L_{ij}^\dagger \,, \tag{12}$$

where $L^\dagger$ is the Moore-Penrose pseudo inverse of L.

Proof. When a unit current is injected at node i and extracted at node j the current-balance equations are $I = e_i - e_j = LV$ or $V = L^\dagger(e_i - e_j)$. The effective resistance r_{ij}^{eff} defined as the potential difference between nodes i and j, $r_{ij}^{\text{eff}} = (e_i - e_j)^T V$, can then be obtained via the impedance matrix $L^\dagger$ as

$$r_{ij}^{\text{eff}} = (e_i - e_j)^T V = (e_i - e_j)^T L^\dagger (e_i - e_j) = L_{ii}^\dagger + L_{jj}^\dagger - 2L_{ij}^\dagger \,,$$

where we have used the fact that the Moore-Penrose inverse of a Laplacian matrix is again a symmetric matrix (see exercise E6.7) and thus $L_{ij}^\dagger = L_{ji}^\dagger$ for all $i, j \in \{1, \dots, n\}$. □

Often it is more convenient to work with a regular matrix and its inverse rather than the singular Laplacian L and its pseudo-inverse $L^\dagger$. We can give an alternative formula to compute the effective resistance based on a regularized Laplacian matrix.

Lemma 5.3 (**Effective resistance from a regular matrix**). *Consider an undirected, connected, and weighted graph with Laplacian $L \in \mathbb{R}^{n \times n}$, and define the matrix $Q = L + \frac{1}{n}\mathbb{1}_n\mathbb{1}_n^T$. The matrix Q is regular and the effective resistance (12) satisfies*

$$r_{ij}^{\text{eff}} = (e_i - e_j)^T Q^{-1} (e_i - e_j) = Q_{ii}^{-1} + Q_{jj}^{-1} - 2Q_{ij}^{-1} \,, \tag{13}$$

Proof. Recall the following identity from Exercise E6.8 (or derive it immediately from the singular value decomposition; see Exercise 15):

$$L^\dagger + \frac{1}{n}\mathbb{1}_n\mathbb{1}_n^T = \left(L + \frac{1}{n}\mathbb{1}_n\mathbb{1}_n^T\right)^{-1} = Q^{-1} \,.$$

We multiply the above equation from the left by $(e_i - e_j)^T$ and from the right by $(e_i - e_j)$. Since $(e_i - e_j)^T\mathbb{1}_n\mathbb{1}_n^T = \mathbb{0}_n^T$, we arrive at $r_{ij}^{\text{eff}} = (e_i - e_j)^T L^\dagger (e_i - e_j) = (e_i - e_j)^T Q^{-1} (e_i - e_j)$. □

The effective resistance is sometimes also referred to as the *resistance distance* [7] since it defines a proper distance metric on a graph, that is, it is a symmetric and nonnegative map from $\mathcal{V} \times \mathcal{V}$ to $\mathbb{R}_{\geq 0}$ that satisfies the triangle inequality.

Lemma 5.4 (**Effective resistance is a distance**). *The effective resistance of an undirected, connected, and weighted graph satisfies*

1. *non-negativity:* $r_{ij}^{\text{eff}} \geq 0$ *for all* $i, j \in \{1, \ldots, n\}$ *and* $r_{ij}^{\text{eff}} = 0$ *if and only if* $i = j$,
2. *symmetry:* $r_{ij}^{\text{eff}} = r_{ji}^{\text{eff}}$ *for all* $i, j \in \{1, \ldots, n\}$, *and*
3. *triangle inequality:* $r_{ij}^{\text{eff}} \leq r_{ik}^{\text{eff}} + r_{kj}^{\text{eff}}$ *for all* $i, j, k \in \{1, \ldots, n\}$,

that is, the effective resistance is a proper distance metric.

The proof of Lemma 5.4 is deferred to Exercise 5.

Another important property of the effective resistance is *Rayleigh's monotonicity law*:

"The effective resistances are monotone functions of the branch resistances."

We will state Rayleigh's monotinicity law in the language of algebraic graph theory below.

Lemma 5.5 (**Rayleigh's monotonicity law**). *Consider two symmetric and irreducible adjacency matrices* $A, \tilde{A} \in \mathbb{R}^{n \times n}$ *corresponding to two undirected, connected, and weighted graphs with identical node sets but possibly different edge sets and edge weights. Consider the associated matrices of effective resistances* $R^{\text{eff}}, \tilde{R}^{\text{eff}} \in \mathbb{R}^{n \times n}$. *If* $\tilde{a}_{ij} \geq a_{ij}$ *for all* $i, j \in \{1, \ldots, n\}$, *then* $\tilde{r}_{ij}^{\text{eff}} \leq r_{ij}^{\text{eff}}$ *for all* $i, j \in \{1, \ldots, n\}$.

Proof. We will prove Rayleigh's monotonicity law by appealing to a classic circuit-inspired proof technique [5]. The circuits associated with the graphs induced by A and $\tilde{A}$ have branch resistances $r_{ij} = 1/a_{ij} \geq 0$ and $\tilde{r}_{ij} = 1/\tilde{a}_{ij} \geq 0$, where $\tilde{r}_{ij} \leq r_{ij}$ since $\tilde{a}_{ij} \geq a_{ij}$. Observe that a non-existing edge $\{i, j\} \notin \mathcal{E}$ with $a_{ij} = 0$ corresponds to a infinite resistance $r_{ij} = \infty$ which is consistent with our intuition. We denote the current flows in both circuits by f_{ij} and $\tilde{f}_{ij}$ for all $\{i, j\} \in \mathcal{E}$.

We first show an energy interpretation of the effective resistance. Consider a unit current injection at node i and a unit current extraction at node j. Then the current-balance equations are $I = e_i - e_j = LV$, and the effective resistance r_{ij}^{eff} defined as the potential difference $(e_i - e_j)^T V$ between nodes i and j can be manipulated as follows:

$$r_{ij}^{\text{eff}} = (e_i - e_j)^T V = V^T L V = \frac{1}{2} \sum\nolimits_{i,j=1}^{n} \frac{1}{r_{ij}} (V_i - V_j)^2 = \frac{1}{2} \sum\nolimits_{i,j=1}^{n} r_{ij} f_{ij}^2.$$

Thus, when a unit current injection at node i and a unit current extraction at node j, the effective resistance r_{ij}^{eff} equals the energy dissipated in the network branches. The same reasoning applies to the effective resistances $\tilde{r}_{ij}^{\text{eff}}$ in the other network. Recall also the Thompson principle from exercise E6.13 which states that the flows $f_{ij} = \frac{1}{r_{ij}}(V_i - V_j)$ are the unique branch flows that minimize the energy dissipation $\frac{1}{2} \sum_{i,j=1}^{n} r_{ij} f_{ij}^2$ in the network.

By using the energy interpretation of the effective resistance, the Thompson principle, and our starting assumption $\tilde{r}_{ij} \leq r_{ij}$, we obtain the claimed monotonicity law:

$$\tilde{r}_{ij}^{\text{eff}} = \frac{1}{2} \sum\nolimits_{i,j=1}^{n} \tilde{f}_{ij}^2 \tilde{r}_{ij} \leq \frac{1}{2} \sum\nolimits_{i,j=1}^{n} \tilde{f}_{ij}^2 r_{ij} \leq \frac{1}{2} \sum\nolimits_{i,j=1}^{n} f_{ij}^2 r_{ij} = r_{ij}^{\text{eff}}.$$

□

We refer to the quantity

$$R_{\text{tot}} = \sum_{i,j=1,i<j}^{n} r_{ij}^{\text{eff}} \tag{14}$$

as the *total effective resistance* of the graph (or sometimes also as the Kirchoff index). In view of Lemma 5.4, the effective resistance is a distance measure. Thus, the reciprocal of the total effective resistance, $1/R_{\text{tot}}$, should be a graph connectivity metric similar to the second-smallest Laplacian eigenvalue, the algebraic connectivity λ_2. The following result relates the Laplacian eigenvalues including the algebraic connectivity to the total effective resistance.

Lemma 5.6 (**Total effective resistance and Laplacian eigenvalues).** *Consider an undirected, connected, and weighted graph, its Laplacian matrix $L \in \mathbb{R}^{n\times n}$ with Laplacian spectrum* $\text{spec}(L) = \{0, \lambda_2, \dots, \lambda_n\}$*, its effective resistances r_{ij}^{eff} in (11) for all $i, j \in \{1, \dots, n\}$, as well as the total effective resistance R_{tot} in (14). It holds that*

$$R_{\text{tot}} = \sum_{i,j=1,i<j}^{n} r_{ij}^{\text{eff}} = n \sum_{i=2}^{n} \frac{1}{\lambda_i}\,.$$

Proof. In vector form, the matrix of effective resistances r_{ij}^{eff} can be calculated according to (12) as

$$R = \Big(\text{diag}(L^\dagger)\mathbb{1}_n\Big)\,\mathbb{1}_n^T + \mathbb{1}_n\,\Big(\mathbb{1}_n^T \text{diag}(L^\dagger)\Big) - 2L^\dagger\,,$$

where we used the shorthand $\text{diag}(L^\dagger) = \text{diag}(L_{ii}^\dagger)$ reducing $L^\dagger$ to its diagonal entries. Thus, the total effective resistance (14) evaluates to

$$\begin{aligned} R_{\text{tot}} =& \frac{1}{2}\mathbb{1}_n^T R \mathbb{1}_n \\ =& \frac{1}{2}\mathbb{1}_n^T \text{diag}(L^\dagger)\mathbb{1}_n \mathbb{1}_n^T\mathbb{1}_n + \frac{1}{2}\mathbb{1}_n^T\mathbb{1}_n\mathbb{1}_n^T \text{diag}(L^\dagger)\mathbb{1}_n - \mathbb{1}_n^T L^\dagger \mathbb{1}_n \\ =& n \cdot \mathbb{1}_n^T \text{diag}(L^\dagger)\mathbb{1}_n = n \cdot \text{trace}(L^\dagger) = n\sum_{i=2}^{n}\frac{1}{\lambda_i}\,, \end{aligned}$$

where we used that $L^\dagger\mathbb{1}_n = \mathbb{0}_n$ (see exercise E6.7), $\mathbb{1}_n^T\mathbb{1}_n = n$, and the fact that $\text{trace}(L^\dagger)$ is the sum of eigenvalues of $L^\dagger$ which is the sum of the reciprocals of the nonzero Laplacian eigenvalues. □

Note that the effective resistance is thus proportional to the $\mathcal{H}_2$ norm of a Laplacian flow as identified in exercise E10.5. Hence, just like the algebraic connectivity quantifies the worst-case decay rate of a Laplacian flow, the total effective resistance quantifies an average performance metric in terms of the $\mathcal{H}_2$ norm. Additionally, just like the algebraic connectivity is a monotone function of the edge weights (see Exercise E6.9), the total effective resistance enjoys this property as well by Rayleigh's monotonicity law.

We refer to [5, 10, 7, 6, 3, 1] for further reading on the properties of the effective resistance and its connections to random walks, network dynamics, as well as distributed control and estimation.

6 Circuit reduction

Every scholar of engineering is familiar with the reduction of a circuit composed of a series of two resistors to a single resistor, as depicted in Figure 6. Another well-know circuit reduction is the

transformation of a cyclic Δ-circuit to an acyclic Y-circuit akin the to the $\Delta - Y$-transformation, as depicted in Figure 7. In the following, we will analyze this reduction process, termed *Kron reduction* [8] after the engineer Gabriel Kron, from the viewpoint of algebraic graph theory.

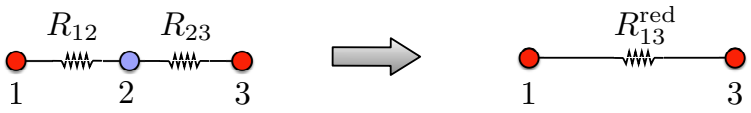

Figure 6: Reduction of a resistive series circuit to a single resistor with value $R_{13}^{\text{red}} = R_{12} + R_{23}$

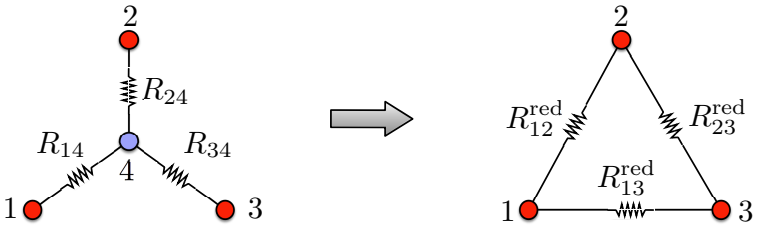

Figure 7: Reduction of a resistive and cyclic Δ-circuit to an acyclic Y-circuit with resistances $R_{23}^{\text{red}} = \frac{R_{14}R_{34}+R_{34}R_{24}+R_{24}R_{14}}{R_{14}}$, $R_{12}^{\text{red}} = \frac{R_{14}R_{34}+R_{34}R_{24}+R_{24}R_{14}}{R_{34}}$, and $R_{13}^{\text{red}} = \frac{R_{14}R_{34}+R_{34}R_{24}+R_{24}R_{14}}{R_{24}}$.

Consider a connected and resistive circuit partitioned with nodes $\mathcal{V} = \{1, \dots, n\}$ into two sets of $\mathcal{V} = \mathcal{V}_1 \cup \mathcal{V}_2$ that we term boundary nodes and interior nodes (depicted as red and blue nodes in Figures 6 and 7). The associated partitioned current-balance equations are

$$\left[\begin{array}{c} I_1 \\ \hline I_2 \end{array}\right] = \left[\begin{array}{c|c} L_{11} & L_{12}^T \\ \hline L_{12} & L_{22} \end{array}\right] \left[\begin{array}{c} V_1 \\ \hline V_2 \end{array}\right], \tag{15}$$

where $L = L^T$ is the associated conductance matrix — an irreducible Laplacian matrix satisfying $L\mathbb{1}_n = \mathbb{0}_n$ — and the external current injections $I \in \mathbb{R}^n$ are balanced: $\mathbb{1}_n^T I = 0$. Observe that the lower-right block L_{22} is a loopy Laplacian matrix and thus non-singular; see Exercise 10.

By eliminating the voltages V_2 of the interior nodes as $V_2 = L_{22}^{-1} I_2 - L_{22}^{-1} L_{12}^T V_1$, we obtain

$$\underbrace{I_1 - L_{12}L_{22}^{-1}I_2}_{I^{\text{red}}} = \underbrace{\left(L_{11} - L_{12}L_{22}^{-1}L_{12}^T\right)}_{L^{\text{red}}} V_1 \,. \tag{16}$$

In the following, we will establish that the reduced equations (16) are indeed well-defined circuit equations, as suggested by the examples in Figures 6 and 7.

Lemma 6.1 (Kron reduction). *Consider the resistive circuit equations (15) parameterized by the irreducible conductance matrix satisfying $L\mathbb{1}_n = \mathbb{0}_n$ and the balanced current injections $I \in \mathbb{R}^n$ satisfying $\mathbb{1}_n^T I = 0$. Consider also the associated reduced circuit equations (16) parameterized by $I^{\text{red}} = I_1 - L_{12}L_{22}^{-1}I_2$ and $L^{\text{red}} = L_{11} - L_{12}L_{22}^{-1}L_{12}^T$. The following statements hold:*

1. *The matrix $-L_{12}L_{22}^{-1}$ is nonnegative and column-stochastic, and the reduced current injections $I^{\text{red}} = I_1 - L_{12}L_{22}^{-1}I_2$ are balanced: $\mathbb{1}^T I^{\text{red}} = 0$.*

2. *The reduced conductance matrix $L^{\text{red}} = L_{11} - L_{12}L_{22}^{-1}L_{12}^T$ is a nonnegative, symmetric, and irreducible Laplacian matrix satisfying $L^{\text{red}}\mathbb{1} = \mathbb{0}$.*

3. *The graph associated to the Laplacian L^{red} has an edge between nodes $i, j \in \mathcal{V}_1$ if and only if*

(i) either $\{i, j\}$ was an edge in the original graph associated to L,

(ii) or there was a path $\{i, k_1, \ldots, k_m, j\}$ in the original graph between nodes i and j passing through only interior nodes $k_1, \ldots, k_m \in \mathcal{V}_2$.

Proof. We prove Lemma 6.1 by subsequently eliminating one boundary node at a time, and show that the three claimed properties hold, i.e., the Laplacian and current balance properties remain preserved. Consider a removal of the nth voltage (observe that $L_{nn} \neq 0$ due to irreducibility) as

$$V_n = \frac{1}{L_{nn}} \left(I_n - \sum_{j=1}^{n-1} L_{jn} V_j \right) .$$

In this case, the current balance equation $I = LV$ simplifies to

$$\begin{bmatrix} I_1 \\ \vdots \\ I_{n-1} \end{bmatrix} + \underbrace{\begin{bmatrix} -L_{1n}/L_{nn} \\ \vdots \\ -L_{n-1,n}/L_{nn} \end{bmatrix}}_{=A} I_n = \underbrace{\begin{bmatrix} \ddots & \vdots & \iddots \\ \ldots & L_{ij} - \frac{L_{in} \cdot L_{jn}}{L_{nn}} & \ldots \\ \iddots & \vdots & \ddots \end{bmatrix}}_{=B} \begin{bmatrix} V_1 \\ \vdots \\ V_{n-1} \end{bmatrix} , \tag{17}$$

where the (i, j)-element of B is given by $B_{ij} = L_{ij} - L_{in} \cdot L_{jn}/L_{nn}$. In the following, we will prove the claimed three properties for the A and B matrices.

With regards to the properties of A, observe that $L_{nn} > 0$ and $-L_{in} \geq 0$ for all $i \in \{1, \ldots, n-1\}$. Thus, A is non-negative. At least one element of A is strictly positive since at least one $-L_{in} > 0$ due to irreducibility: at least one node $i \in \{1, \ldots, n-1\}$ is connected to node n. Moreover,

$$\sum_{i=1}^{n-1} A_i = -\sum_{i=1}^{n-1} L_{in}/L_{nn} = -(-L_{nn}/L_{nn}) = 1 ,$$

where we used the fact that L has zero row and column sums. Hence, the matrix A (corresponding to the matrix $-L_{12}L_{22}^{-1}$ in the lemma) is nonnegative and column-stochastic. Thus, the overall current balance is preserved in the equations (17):

$$\mathbb{1}_{n-1}^T \begin{bmatrix} I_1 \\ \vdots \\ I_{n-1} \end{bmatrix} + \mathbb{1}_{n-1}^T A I_n = \mathbb{1}_{n-1}^T \begin{bmatrix} I_1 \\ \vdots \\ I_{n-1} \end{bmatrix} + I_n = \mathbb{1}_n I = 0 .$$

With regards to the properties of B, we first analyze the off-diagonal elements for $i \neq j$:

$$B_{ij} = \underbrace{L_{ij}}_{< 0 \text{ if } \{i,j\} \in \mathcal{E} \text{ and } = 0 \text{ else}} - \underbrace{L_{in} \cdot L_{jn}/L_{nn}}_{> 0 \text{ if } \{i,n\},\{n,j\} \in \mathcal{E} \text{ and } = 0 \text{ else}}$$

We conclude that $B_{ij} \leq 0$ always holds, and $B_{ij} < 0$ if and only if either $\{i, j\}$ was an edge in the original graph associated to L, or there was a path $\{i, n, j\}$ in the original graph between nodes i and j passing through the eliminated node n. Next, we analyze the row sums of B given by

$$\sum\nolimits_{j=1}^{n-1} B_{ii} = \sum\nolimits_{j=1}^{n-1} L_{ij} - \frac{L_{in} \cdot L_{jn}}{L_{nn}} = \sum\nolimits_{j=1}^{n-1} L_{ij} - \frac{L_{in}}{L_{nn}} \sum\nolimits_{j=1}^{n-1} L_{jn} = -L_{in} - \frac{L_{in}}{L_{nn}}(-L_{nn}) = 0 ,$$

where we used that the row and column sums of L are zero. We conclude that B has non-positive diagonals, zero row sums, zero column sums (due to symmetry), and thus also positive diagonal elements. Hence, B is a Laplacian matrix that induces a topology as in the third claimed property.

Hence, we have proved the three properties of the lemma for a single reduction step, and showed that the reduced equations (17) can still be associated to a circuit, that is, the Laplacian property and the balanced current injections are preserved by iterating these arguments for the elimination of one boundary node at a time, we arrive at the claimed statement. □

Observe that due to the third property of Lemma 6.1 the graph associated to the Kron-reduced network is always *denser* than the original graph. These results can also be adapted to the case when the network features resistive loads; see Exercise 16. We refer to [3] for further interesting properties of Kron reduction and its connection to other concepts such as the effective resistance.

7 Control of DC power grids

Consider a direct current (DC) power grid with modeled by a circuit with n nodes of which n_L are loads and $n_S = n - n_L$ are controllable sources which we denote by the sets L and S, respectively. The circuit consists of m resistive lines with resistors r_{ij}, incidence matrix $B \in \mathbb{R}^{n\times m}$, admittance (Laplacian) matrix $L = B\mathrm{diag}(1/r_{ij})B^T$, constant current loads $I^L \in \mathbb{R}^{n_L}_{\leq 0}$, and controllable sources $I^S \in \mathbb{R}^{n_S}$. The governing circuit equations are as in (1)

$$\begin{bmatrix} I^S \\ I^L \end{bmatrix} = \begin{bmatrix} L_{SS} & L_{SL} \\ L_{LS} & L_{LL} \end{bmatrix} \begin{bmatrix} V^S \\ V^L \end{bmatrix}, \tag{18}$$

where we partitioned the circuit equations according to sources and loads, and V^S and V^L are the respective vectors of nodal voltages. By multiplying the circuit equations (18) from the left by $\mathbb{1}_n^T$ we obtain the balance of external injections

$$\mathbb{1}_{n_S}^T I^S + \mathbb{1}_{n_L}^T I^L = 0\,. \tag{19}$$

Observe that the balance of sources and loads in (19) is a necessary condition for feasibility of the equations (18). However, unless the loads I^L are directly measured, or at least the overall load $\mathbb{1}_{n_L}^T I^L$ is measured, it is not possible to schedule the sources I^S accordingly so that (19) is satisfied.

In order to learn the overall load balance, we attach a dynamic controller to every node as

$$I_i^S = I_i^{\mathrm{ref}} - c_i \dot{V}_i\,, \quad i \in S\,, \tag{20}$$

where $I^{\mathrm{ref}} \geq 0$ is a vector of nominal current injection and $c_i > 0$ is a control gain. From a circuit perspective, the controller (20) corresponds to adding a capacitance c_i to ground as well as a constant current injection I_i^{ref} to each source; see Figure 8 for an analog circuit realization of (20).

Theorem 7.1 (Convergence of voltage drifts). *Consider the DC power grid model (18) with the feedback controller (20). All voltage drifts asymptotically synchronize as*

$$\lim_{t\to\infty} \dot{V}(t) = \dot{V}_{\mathrm{drift}} \mathbb{1}_n = \frac{\mathbb{1}_{n_S}^T I^{\mathrm{ref}} + \mathbb{1}_{n_L}^T I^L}{\mathbb{1}_{n_S}^T C \mathbb{1}_{n_S}} \mathbb{1}_n\,. \tag{21}$$

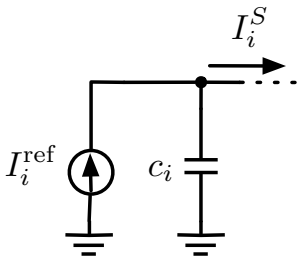

Figure 8: Circuit realization of the controller (20)

Proof. The closed-loop system (18),(20) is given by

$$\begin{bmatrix} C\dot{V}^S \\ \mathbb{0}_{n_L} \end{bmatrix} = \begin{bmatrix} I^{\text{ref}} \\ I^L \end{bmatrix} - \begin{bmatrix} L_{SS} & L_{SL} \\ L_{LS} & L_{LL} \end{bmatrix} \begin{bmatrix} V^S \\ V^L \end{bmatrix}, \tag{22}$$

where $C = \text{diag}(c_i)$. Assume that there is a solution to system (22) with a common synchronized voltage drift that satisfies $\dot{V}(t) = \dot{V}^*(t)\mathbb{1}_n$, where $\dot{V}^*(t) \in \mathbb{R}$ is a scalar signal. Then by inserting this hypothetical solution into (22) and multiplying this equation from the left by $\mathbb{1}_n^T$ we obtain

$$\mathbb{1}_{n_S}^T C \mathbb{1}_{n_S} \cdot \dot{V}^*(t) = \mathbb{1}_{n_S}^T I^{\text{ref}} + \mathbb{1}_{n_L}^T I^L .$$

Hence, if a solution with synchronized voltage drifts $\dot{V}^*(t) \in \mathbb{R}$ exists, then $\dot{V}^*(t)$ must take the *constant* value $\dot{V}_{\text{drift}}$ as claimed in (21). To show that this solution with synchronized voltage drifts actually exists and is asymptotically stable, define $(x(t), y(t)) = (\dot{V}^S(t), \dot{V}^L(t))$. By taking one more derivative of the closed loop (22), we obtain the consensus-type system

$$\begin{bmatrix} C\dot{x} \\ \mathbb{0}_{n_L} \end{bmatrix} = - \begin{bmatrix} L_{SS} & L_{SL} \\ L_{LS} & L_{LL} \end{bmatrix} \begin{bmatrix} x \\ y \end{bmatrix} . \tag{23}$$

System (23) consists of coupled differential equations in the variable x and algebraic equations in the variable y. To construct a system of pure differential equations, we perform successive Gaussian elimination of the algebraic variables $(y_1, y_2, \ldots, y_{n_L})$. Observe that the matrix $L \in \mathbb{R}^{n \times n}$ in (23) is a symmetric and irreducible Laplacian matrix. Recall from Lemma 6.1 that successive Gaussian elimination of each the y-variables renders the Laplacian matrix L into new matrix (of smaller dimension) that is also a symmetric and irreducible Laplacian matrix. Thus, an elimination of all algebraic variables $(y_1, y_2, \ldots, y_{n_L})$ results in the system

$$C\dot{x} = -L_{\text{red}} x , \tag{24}$$

where $L_{\text{red}} \in \mathbb{R}^{n_S \times n_S}$ is a symmetric and irreducible Laplacian matrix[1]. Observe that system (24) is a standard directed consensus system with Laplacian $C^{-1}L_{\text{red}}$ associated to a strongly connected and bidirectional graph with non-symmetric weights. By Theorem 7.3, we have $x(t \to \infty) = x^* \mathbb{1}_{n_S}$ where x^* is a constant depending on the initial conditions. Observe that if $x(t \to \infty) = x^* \mathbb{1}_{n_S}$, then from equation (23) we must also have that $y(t \to \infty) = x^* \mathbb{1}_{n_L}$. Hence, all solutions $(x(t), y(t)) = (\dot{V}^S(t), \dot{V}^L(t))$ converge to the voltage drift $x^* \mathbb{1}_n$ which is given in (21). □

[1] A Gaussian elimination of the y-variables in (23) reads in vector form as $y = -L_{LL}^{-1} L_{LS} x$, where we recall from Exercise 10 that L_{LL} is positive definite and nonsingular. Thus, L_{red} in (24) reads as $L_{\text{red}} = L_{SS} - L_{SL} L_{LL}^{-1} L_{LS}$.

Observe that the common voltage drift $\dot{V}_{\text{drift}}$ under the controller (20) reveals the total imbalance of the total nominal source injections $\mathbb{1}_{n_S}^T I^{\text{ref}}$ and the total load $\mathbb{1}_{n_L}^T I^L$. Thus, a negative (respectively, positive) value of the drift $\dot{V}_{\text{drift}}$ indicates that further (respectively, less) currents must be injected by the sources. This motivates the following simple decentralized controller that aside from the control action (20) additionally integrates the locally measured voltage drift:

$$\begin{aligned} I_i^S &= I_i^{\text{ref}} - c_i \dot{V}_i - p_i \\ k_i \dot{p}_i &= \dot{V}_i \,, \end{aligned} \tag{25}$$

where $k_i > 0$ and $i \in S$. As it turns out the decentralized controller (25) is able to balance generation and load by means of the additional injection $-p_i$ at every source.

Theorem 7.2 (**Decentralized generation/load balancing**). *Consider the DC power grid model (18) with the control input (25). All voltages asymptotically converge to constant values and all injections are balanced:*

$$\mathbb{1}_{n_S}^T I^{\text{ref}} + \mathbb{1}_{n_L}^T I^L = \mathbb{1}_{n_S}^T p(t \to \infty) \,. \tag{26}$$

Proof. The closed-loop system (18),(25) is given by

$$\begin{aligned} \begin{bmatrix} C\dot{V}^S \\ \mathbb{0}_{n_L} \end{bmatrix} &= \begin{bmatrix} I^{\text{ref}} - p \\ I^L \end{bmatrix} - \begin{bmatrix} L_{SS} & L_{SL} \\ L_{LS} & L_{LL} \end{bmatrix} \begin{bmatrix} V^S \\ V^L \end{bmatrix} \\ K\dot{p} &= \dot{V}^S \,, \end{aligned} \tag{27}$$

where $K = \text{diag}(k_i)$ is positive definite. Observe that if the system (27) features an equilibrium with $\dot{p} = \dot{V}^S = \mathbb{0}_{n_S}$, then a multiplication of the steady-state equations (27) from the left by $\begin{bmatrix} \mathbb{1}_n^T & \mathbb{0}_{n_S}^T \end{bmatrix}$ yields the load/generation balance (26). In the following, we show that system (27) indeed admits a steady state. An equivalent formulation of the controller (25) is obtained by integrating $k_i \dot{p}_i = \dot{V}_i^S$:

$$I_i^S = I_i^{\text{ref}} - c_i \dot{V}_i - \frac{1}{k_i}(V_i - V_i(0)) - p_i(0) \,, \quad i \in S \,. \tag{28}$$

With the formulation (32), the closed loop (27) simplifies to

$$\begin{bmatrix} C\dot{V}^S \\ \mathbb{0}_{n_L} \end{bmatrix} = \begin{bmatrix} I^{\text{ref}} + \frac{1}{k_i} V_i(0) - p_i(0) \\ I^L \end{bmatrix} - \begin{bmatrix} L_{SS} + K^{-1} & L_{SL} \\ L_{LS} & L_{LL} \end{bmatrix} \begin{bmatrix} V^S \\ V^L \end{bmatrix} .$$

As in the proof of Theorem 7.1, by successively eliminating the algebraic variables V^L, we obtain the reduced system

$$C\dot{V}^S = -(L_{\text{red}} + K^{-1})V^S + \left(I^{\text{ref}} + \frac{1}{k_i} V_i(0) - p_i(0) - L_{SL} L_{LL}^{-1} I^L \right) , \tag{29}$$

where L_{red} is the same symmetric and irreducible Laplacian matrix as in (24). System (29) is linear with constant input term and system matrix $A = -C^{-1}(L_{\text{red}} + K^{-1})$, where $L_{\text{red}} \in \mathbb{R}^{n_S \times n_S}$ is a symmetric and irreducible Laplacian matrix. Observe that the matrix $L_{\text{red}} + K^{-1}$ is positive definite, see Exercise 10. Hence, the Lyapunov equation $PA + A^T P = Q$ is fulfilled with positive definite matrices $P = C$ and $Q = (L_{\text{red}} + K^{-1})$. We conclude that the system (29) converges to an exponentially stable equilibrium and the claim follows. □

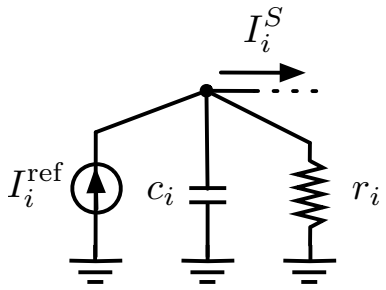

Figure 9: Circuit realization of the controller (25)

The equivalent formulation (32) of the controller (25) admits again (up to initial values) an analog circuit realization shown in Figure 9. In conclusion, the decentralized controller (25) learns the overall load/generation balance and asymptotically compensates for the unknown loading in (26). However, the decentralized controller (25) may suffer from robustness issues (see Exercise 9) which is why distributed control strategies involving communication between the controllers are preferred similar to the PI consensus controller in Exercise E8.4 (see Exercise 11).

In alternating current (AC) power networks, the above control strategies (20) and (25) are often referred to as primary droop control and secondary integral control, respectively. They provide the basis for operation of an AC power grid. We refer to [11] for further details on the operation of DC power grids using consensus strategies, and to [4] regarding their extensions to AC networks.

8 Exercises

1. Exercise 1 **(Special circuit models)**: Consider the circuit model (6). Your task is to derive some special instances under certain assumptions.

   a) Assume the absence of constant current injections and dissipative elements, that is, $I^* = \mathbb{0}_n$, $G = \mathbb{0}$ and $R = \mathbb{0}$. Show that, under these assumptions and for $C = I_n$, the circuit equations (3) reduce to the Laplacian oscillator (5).

   b) Assume homogeneous L/R ratios. that is, $l_{ij}/r_{ij} = \tau$ is constant for all edges $\{i, j\} \in \mathcal{E}$. Derive the second-order consensus-type model (6).

2. Exercise 2 **(Circuit with partial dissipation)**: Consider the circuit model (4) without external current injections: $I^* = \mathbb{0}_n$. In the following we study the equilibria of the system when the underlying graph is connected and either $G = \mathbb{0}$ or $R = \mathbb{0}$:

   a) Show that for $R = \mathbb{0}$ and G is positive definite, equilibria are defined uniquely up to a subspace corresponding to currents circulating in the network: $(V^*, f^*) \in (\mathbb{0}_n, \text{kernel}(B))$.

   b) Show that for $G = \mathbb{0}$ and R is positive definite, equilibria are defined uniquely up to to a subspace corresponding to voltages reaching consensus: $(V^*, f^*) \in (\text{span}(\mathbb{1}_n), \mathbb{0}_m)$.

   c) Show that the equilibria found in a) and b) are asymptotically stable.
   (*Hint:* try to apply Lemma 7.5. or an analysis via energy functions)

   d) How would you modify these proofs for $I^* \neq \mathbb{0}_n$ Would you still reach a steady-state ?

3. Exercise 3 **(Parallel RL branch dynamics)**: Repeat the analysis in Section 4 for the case that the branch dynamics (3d) are given by a parallel connection of resistive and inductive elements.

4. Exercise 4 **(Mechanical analog)**: Provide a mechanical analog of the circuit model (3) using masses, springs, and dampers.

5. Exercise 5 **(Resistance distance)**: Prove Lemma 5.4 and show that the effective resistance is a distance measure.

6. Exercise 6 **($\mathcal{H}_2$-norm and effective resistance)**: Consider a connected resistive circuit, where each node has a capacitor to ground of unit capacitance. We equip this circuit with inputs and measurement outputs. The inputs are exogenous nodal current injections $I_i^*(t)$, that we assume to be white noise signals affecting each node $i \in \{1, \dots, n\}$. The output is the deviation from voltage consensus $y(t) = (I_n - \mathbb{1}_n \mathbb{1}_n^T/n)V(t)$.

   - Model the circuit by a set of differential equations; and
   - show that the $\mathcal{H}_2$ performance of the circuit dynamics equals the average effective resistance $\frac{1}{n}\sum_{i,j=1,i<j}^{n} r_{ij}^{\text{eff}}$.

7. Exercise 7 **(Control of inductive power grids)**: Extend the results of Theorems 7.1 and 7.2 from a circuit with purely resistive branches to a circuit whose branches are composed of a series $R - L$ circuit with constant ratios r_{ij}/l_{ij} for all $\{i, j\} \in \{1, \dots, n\}$.

8. Exercise 8 **(Load sharing)**: Consider the DC power grid model (18) with the control input (20) as well as a set of positive numbers $w_1, \dots, w_{n_S}$ depicting the rating of the sources. Provide conditions on the control parameters I_i^{ref} and c_i for $i \in \{1, \dots, n\}_S$ so that the source injections are asymptotically shared between sources proportional to their ratings:

$$\frac{I_i^S(t \to \infty)}{I_j^S(t \to \infty)} = \frac{w_i}{w_j}\,, \qquad i, j \in \{1, \dots, n_S\}\,.$$

9. Exercise 9 **(Decentralized integral control with measurement errors)**: Consider the DC power grid model (18) with the decentralized controller (25), and assume that it is implemented by measuring the voltage drift possibly subject to a constant bias

$$\begin{aligned} I_i^S &= I_i^{\text{ref}} - c_i y_i - p_i\,, \\ k_i \dot{p}_i &= y_i\,, \\ y_i &= \dot{V}_i + \eta_i\,, \end{aligned} \tag{30}$$

   where $k_i > 0$ is a gain, y_i is a measurement, and $\eta_i \in \mathbb{R}$ is a measurement drift for each $i \in S$. Show that this system does not admit a steady state (not even a solution with synchronized voltage drifts $\lim_{t\to\infty} \dot{V}(t) = \dot{V}_{\text{drift}} \mathbb{1}_n$) if the measurement biases are not identical. Can you think a possible variation of the integral controller (32) to alleviate this problem?

10. Exercise 10 **(Loopy Laplacian matrices)**: Consider an undirected, connected, and weighted graph $G = (\mathcal{V}, \mathcal{E}, A)$ induced by the nonnegative adjacency matrix $A \in \mathbb{R}^{n\times n}$. In the following, we construct a so-called *loopy Laplacian matrix* [3] that takes self-loops induced by the diagonal elements $a_{ii} \geq 0$ into account. The loopy Laplacian is defined by

$$L_{\text{loopy}} = B\text{diag}(a_{ij})B^T + \text{diag}(a_{ii}).$$

   Show that $L_{\text{loopy}} \in \mathbb{R}^{n\times n}$ is a positive definite matrix as long as at least one element $a_{ii} > 0$ is strictly positive for $i \in \{1, \dots, n\}$.

11. Exercise 11 **(Distributed averaging-based proportional-integral control)**: Consider the DC power grid model (18) with the following distributed averaging-based proportional-integral (DAPI) controller (see Exercise E6.16)

$$\begin{aligned} I_i^S &= I_i^{\mathrm{ref}} - c_i \dot{V}_i - p_i \,, \\ k_i \dot{p}_i &= c_i \dot{V}_i - \sum\nolimits_{j=1}^{n} a_{ij} \left(\frac{p_i}{w_i} - \frac{p_j}{w_j} \right) , \end{aligned} \tag{31}$$

where $k_i > 0$ is a control gain for each $i \in S$, w_i for $i \in S$ are the source ratings from Exercise 8, and the symmetric, nonnegative, and irreducible matrix $A \in \mathbb{R}^{n_S \times n_S}$ with elements $a_{ij} \geq 0$ encodes a communication network between the controllers. Show that the DAPI controller (33) drives the DC power grid model (18) to an asymptotically stable steady state with integral inputs $p(t \to \infty)$ satisfying the fair proportional load sharing conditions (see Exercise 8):

$$\frac{p_i(t \to \infty)}{p_j(t \to \infty)} = \frac{w_i}{w_j} \,, \qquad i, j \in \{1, \ldots, n_S\} \,.$$

12. Exercise 12 **(Mechanical ring oscillator)**: Consider the mass-spring network in Figure 10 consisting of four identical particles constrained to move on a circle. Let these masses in turn be coupled by four identical springs, whose elongation/contraction is also confined to the same circle. We model the system by the elongations $q_i \in \mathbb{R}$, $i \in \{1, \ldots, 4\}$, of the four springs and the linear momenta (product of velocity and mass) $p_i \in \mathbb{R}$, $i \in \{1, \ldots, 4\}$, of the four particles. The system dynamics are then described by

$$\dot{q} = B^\top M^{-1} p \,, \tag{32a}$$

$$\dot{p} = -BKq \,, \tag{32b}$$

where $B \in \mathbb{R}^{4 \times 4}$ is the incidence matrix of the graph, $M = m \cdot I_4$ with $m > 0$ is the mass matrix, and $K = k \cdot I_4$ with $k > 0$ is the spring constant matrix.

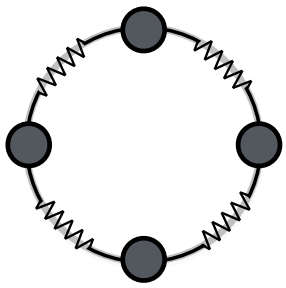

Figure 10: Mechanical ring oscillator

(a) Show that the solution of (36) is a superposition of harmonic signals.

(b) Explicitly calculate the frequencies of these harmonic signals.

13. Exercise 13 **(Resistance identities)**: Let the matrices L, $L^\dagger$, and R represent the Laplacian, pseudo-inverse of the Laplacian, and the effective resistance of an undirected, weighted, and connected graph. Show that:

(a) $L^\dagger R L^\dagger = -2(L^\dagger)^3$,

(b) $L R L = -2 L$.

14. Exercise 14 **(Circuit feasibility)**: Write down a state-space model for the circuit in Figure 11 and verify if it can be put in Laplacian oscillator form.

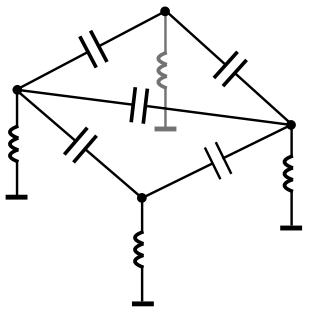

Figure 11: Circuit with capacitors at the edges and inductors to ground at the nodes

15. Exercise 15 **(Regularization of Laplacian matrices)**: Consider a symmetric and irreducible Laplacian matrix $L = L^T \in \mathbb{R}^{n \times n}$. Prove by means of the singular value decomposition that

$$\left(L + \frac{1}{n} \mathbb{1}_n \mathbb{1}_n^T \right)^{-1} = L^\dagger + \frac{1}{n} \mathbb{1}_n \mathbb{1}_n^T .$$

16. Exercise 16 **(Kron reduction in presence of loads)**: Consider a connected and resistive circuit where each node has an associated resistive load modeled as a conductance-to-ground. Consider a partition of the nodes $\mathcal{V} = \{1, \dots, n\}$ into boundary nodes $\mathcal{V}_1$ and interior nodes $\mathcal{V}_2$. The associated current-balance equations are given by

$$\left[\begin{array}{c} I_1 \\ \hline I_2 \end{array}\right] = \left(\left[\begin{array}{c|c} L_{11} & L_{12} \\ \hline L_{12}^T & L_{22} \end{array}\right] + \left[\begin{array}{c|c} G_{11} & \\ \hline & G_{22} \end{array}\right] \right) \left[\begin{array}{c} V_1 \\ \hline V_2 \end{array}\right] ,$$

where G_{11} and G_{22} are diagonal and positive definite matrices associated to the load conductances. Consider now a Kron reduction of the boundary nodes $\mathcal{V}_2$. Investigate how the claimed properties in Lemma 6.1 have to be adapted in this case.

References

[1] P. Barooah and J. P. Hespanha. Estimation from relative measurements: Algorithms and scaling laws. *IEEE Control Systems Magazine*, 27(4):57–74, 2007.

[2] D. S. Bernstein. *Matrix Mathematics*. Princeton University Press, 2 edition, 2009.

[3] F. Dörfler and F. Bullo. Kron reduction of graphs with applications to electrical networks. *IEEE Transactions on Circuits and Systems I: Regular Papers*, 60(1):150–163, 2013.

[4] F. Dörfler, J. W. Simpson-Porco, and F. Bullo. Breaking the Hierarchy: Distributed Control & Economic Optimality in Microgrids. *IEEE Transactions on Control of Network Systems*, 2014. To appear. Available at http://arxiv.org/abs/1401.1767.

[5] P. G. Doyle and J. L. Snell. *Random Walks and Electric Networks*. Mathematical Association of America, 1984.

[6] A. Ghosh, S. Boyd, and A. Saberi. Minimizing effective resistance of a graph. *SIAM Review*, 50(1):37–66, 2008.

[7] D. J. Klein and M. Randić. Resistance distance. *Journal of Mathematical Chemistry*, 12(1):81–95, 1993.

[8] G. Kron. *Tensor Analysis of Networks*. Wiley, 1939.

[9] P. Kundur. *Power System Stability and Control*. McGraw-Hill, 1994.

[10] W. Xiao and I. Gutman. Resistance distance and Laplacian spectrum. *Theoretical Chemistry Accounts*, 110(4):284–289, 2003.

[11] J. Zhao and F. Dörfler. Distributed control and optimization in DC microgrids. *Automatica*, 61:18 – 26, 2015. Available at http://control.ee.ethz.ch/~floriand/docs/Articles/Zhao_Automatica_2015.pdf.